Nanoscale Advances

COMMUNICATION

View Article Online
View Journal | View Issue

Cite this: *Nanoscale Adv.*, 2019, **1**, 4277

Supraparticles with silica protection for redispersible, calcined nanoparticles†

Susanne Wintzheimer, ‡[a] Franziska Miller,‡[a] Johannes Prieschl,[a] Marion Retter[b] and Karl Mandel *[ac]

Received 16th July 2019
Accepted 26th September 2019

DOI: 10.1039/c9na00442d

rsc.li/nanoscale-advances

Calcination of nanoparticles is always accompanied by undesired sintering. A calcination route preventing hard-agglomeration to bulk lumps, which is transferable to almost any kind of metal oxide nanoparticle, is developed by surrounding targeted nanoparticles by silica nanoparticles within a nanostructured microparticle. After calcination, the desired nanoparticles are regained as a monodisperse sol *via* silica dissolution.

Calcination is a heat treatment step which is indispensable for the synthesis or to unfold the desired physical properties of a vast variety of nanoparticles (NPs) including hydroxyapatite ceramics,[1] SnO_2,[2] CeO_2,[3] Cr_2O_3,[4] TiO_2,[5] ZrO_2,[6] Co_3O_4,[7] MgO[8] and Y_2O_3.[9] The calcination process is required to increase the amount of crystalline phase and to decrease crystal defects within the NPs.[2,6] It can promote desired crystal phase conversions and remove unwanted impurities left from synthesis.[2,3,5] Calcination of rare-earth containing crystals enhances their luminescence emission intensity due to a better crystallinity (*i.e.*, less defect states) of the host material, and a better positioning of the rare-earth ions within the crystal lattice.[6,9]

However, it is well-known that calcination of NPs always comes with the unwanted side-effect of sintering, *i.e.*, an increase of crystallite sizes and formation of hard-agglomerates.[2,3,5] This development of solid bridges between particles is extremely disadvantageous as hard-agglomerates cannot be disintegrated by simple means but strong mechanical forces are required to break them down to smaller entities.[10]

In order to avoid sintering, NPs can be protected by a silica coating[11–15] or encapsulation,[16] which is applied *e.g. via* a Stöber process onto the particle surfaces.[17] An alternative approach is to embed NPs in a silica-based hybrid gel.[18] In all cases, the sinter-resistant silica encages the more temperature-labile core material thus preventing its sintering.[19] This has already shown success in temperature treatments up to 800 °C in the case of Pt or Pd NPs used in catalyst applications.[11,14] As a coating of the NPs can be disadvantageous for their later application, a few research groups have also shown that after heat treatment the silica coating can be removed *via* etching in a strong base.[20,21]

Another approach to protect NPs, such as FePt, against sintering is to intermix them with a much larger proportion of NaCl microparticles. Similar to a silica coating, the NaCl encloses the temperature-labile NPs as matrix, enabling their sinter-free annealing and their retrieval by dissolving NaCl in water.[22]

Based on these insights, in this current work presented herein a route toward the fabrication of calcined NPs was developed using supraparticles[23] as intermediary structures. These micron-sized, hierarchical particles consist of silica NPs and another NP type (*e.g.* CaF_2 or TiO_2), which needs to be protected from sintering during calcination. They are assembled upon self-limited self-assembly[24,25] (SLSA) combined with subsequent spray-drying.[26] This procedure affords high flexibility in terms of building block selection (comparable to a toolbox), *i.e.*, it is possible to readily select the sizes, shapes and material types of the primary particles. It consequently enables the straight forward protection of any desired NP with silica (or other sinter-resistant) NPs in a robust, continuous and upscalable process. This displays a significant advantage over approaches using silica coatings, which have to be developed from scratch for every single targeted NP type and are difficult to upscale. In detail, careful control of wet nanochemistry on a larger scale, *e.g.* aiming for the production of

[a]*University Würzburg, Chair of Chemical Technology of Materials Synthesis, Röntgenring 11, 97070 Würzburg, Germany. E-mail: karl-sebastian.mandel@isc.fraunhofer.de*

[b]*Translational Center Regenerative Therapies, TLZ-RT, Fraunhofer Institute for Silicate Research, ISC, Neunerplatz 2, 97082 Würzburg, Germany*

[c]*Fraunhofer Institute for Silicate Research, ISC, Neunerplatz 2, 97082 Würzburg, Germany*

† Electronic supplementary information (ESI) available: Photographs of calcined samples with and without silica protection or upstream supraparticle formation, explanation of the structure of binary spray-dried supraparticles, zeta potential curves of NP dispersions, studies of SLSA using TEM and DLS, SEM showing spray-dried supraparticles before and after calcination, and materials and methods description (PDF). See DOI: 10.1039/c9na00442d

‡ These authors contributed equally.

several hundred grams to kilograms of particles, is a true challenge. Nearly any synthesis protocol has to be modified and *e.g.* working with highly diluted dispersions, which becomes necessary to be able to control the process, renders it impractical and unfeasible.

Fig. 1 Similar to foam peanuts, which are used as protectant against mechanical damage in the packaging of fragile products, SiO_2 NPs protect sinter-labile NPs within a supraparticle during calcination.

As a more detailed outline of this issue would be beyond the scope of this article, the interested reader is referred to a detailed discussion on this issue, which was recently published by us.[27]

The obtained supraparticles resemble raspberries in their structure[28] and allow the calcination of the desired NP type. After calcination of the supraparticles, the (non-silica) NPs are regained as monodisperse sol *via* dissolution of the silica components in a strong base. Fig. 1 depicts the principle of this fabrication route using silica NPs as protectant against sintering, which is similar to foam peanuts as protectant against mechanical damage in the packaging of fragile products. However, it should be noted here that a difference between using foam peanuts for transport (as well as the mentioned approaches of embedding NPs in a gel or a salt matrix) and the herein proposed method is the formation of supraparticles instead of simply mixing both nanoparticles types. This brings the advantage of providing a free flowing micropowder sample after calcination (Fig. S1 in the ESI†) and thus, faster dissolution of the silica components due to a better accessibility compared to bulk material.

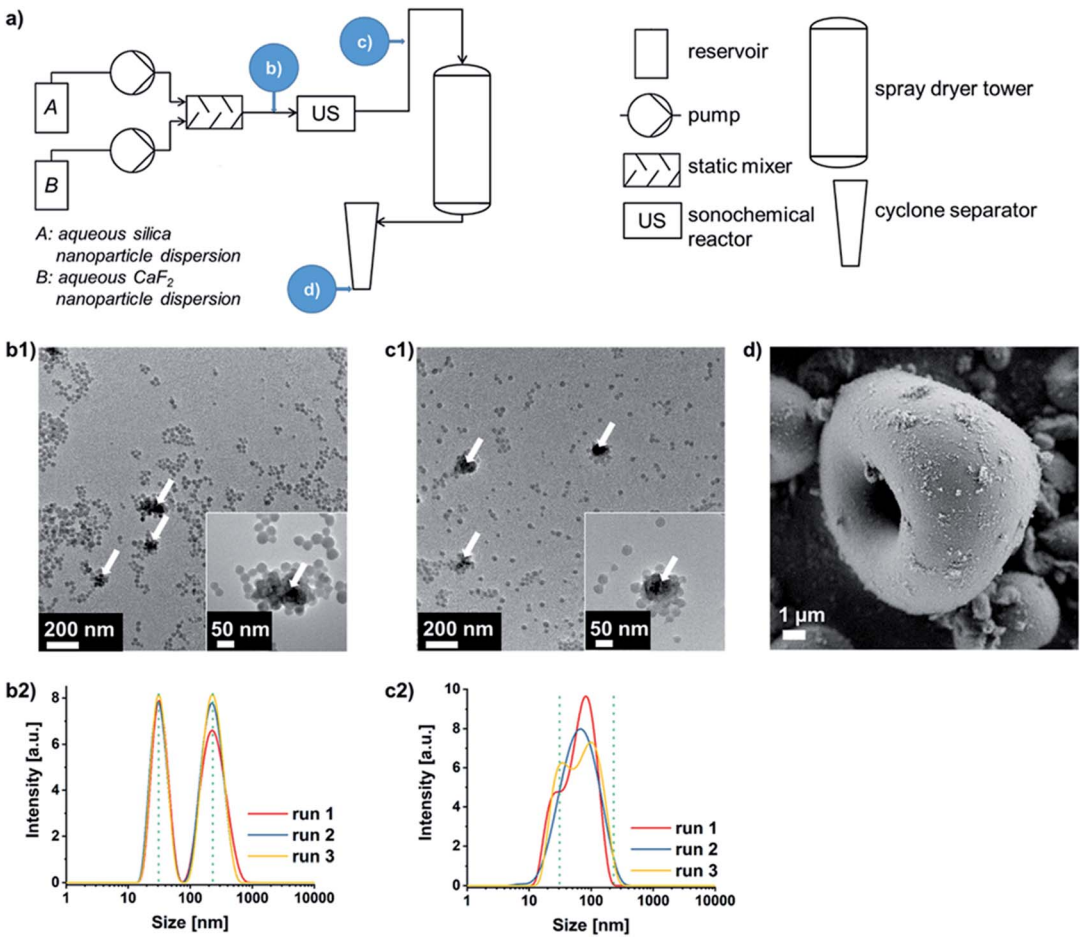

Fig. 2 (a) Schematic process flowsheet of the continuous double assembly process with analyses carried out at different time points (b–d): transmission electron microscopy (TEM) images (b1 and c1, white arrows indicating CaF_2 NPs) and intensity weighted agglomerate sizes determined *via* dynamic light scattering (DLS, b2 and c2) before and after ultrasound-assisted SLSA of the binary NP dispersion, respectively. (d) Scanning electron microscopy after forced assembly of the pre-assembled binary NP dispersion by spray-drying.

In order to optimally protect NPs by silica within a supraparticle during calcination, the spatial separation of sinterlabile NPs from each other is a crucial parameter. This inner structural arrangement of a supraparticle during the kinetic trapping is affected by the number ratio and size ratio of silica to NPs that need to be protected, as well as by the differences in surface charge of both NP types. Several publications have already studied supraparticles made of binary NP dispersions by means of spray-drying assisted assembly.[26,29–31] Based on the findings of these studies, the conclusion can be drawn that for an efficient separation of one particle type by silica, not only silica NPs have to prevail in excess, but also both NP types need to be similar in size (Fig. S2a in the ESI†). This is at least the case for equally charged NPs displaying high surface charges and a good dispersion state in water before spray-drying[29] (Fig. S2b, case I. in the ESI†). However, comparing the surface charge, *i.e.*, the zeta potential of silica with the one of other metal oxide NPs, it appears that the metal oxide NPs usually have their isoelectric points at higher pH values than silica (shown for the samples studied in this work in Fig. S3 in the ESI†).[32]

Thus, obtaining oppositely charged binary dispersions at pH values lying between the isoelectric points of both materials is most practicable in the majority of cases. This is why the concept of so-called SLSA[24] of binary oppositely charged NP

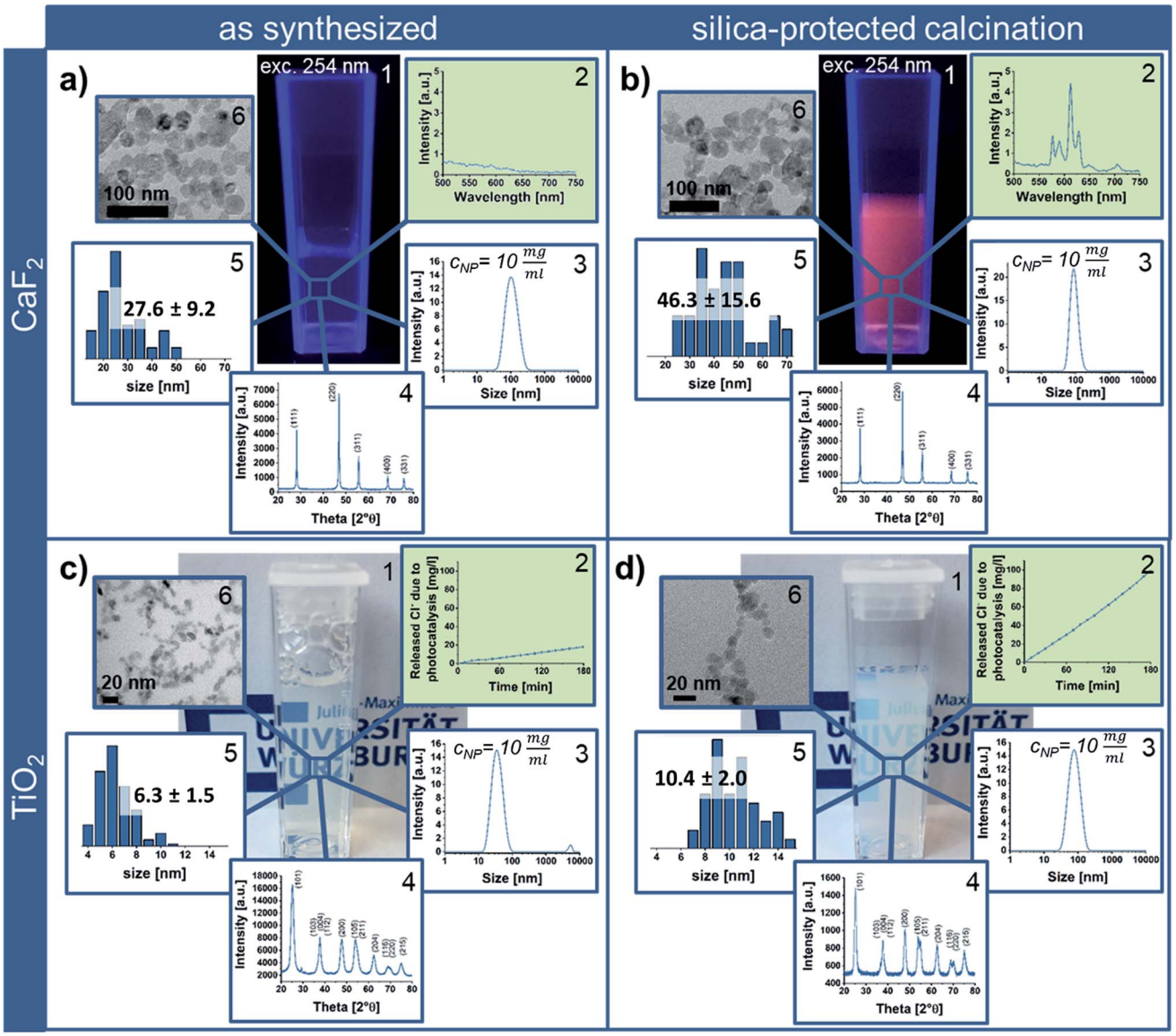

Fig. 3 Eu^{3+} containing CaF_2 (a and b) and anatase NPs (c and d) in the as synthesized state (a and c) compared to calcined samples obtained after silica-protected calcination (which also includes the removal of silica *via* etching and subsequent purification) for 4 h at 600 °C or 800 °C (b and d), respectively. (a) and (b) showing photographs (with UV-light irradiation) (1), photoluminescence spectra (2), intensity weighted agglomerate sizes determined *via* DLS (3; with c_{NP} indicating the sample concentration for measurements), XRD patterns (4) and nanoparticle size and size distribution obtained from TEM images measuring at least 50 particles per sample (5) as well as TEM images (6). (c) and (d) depicts the same analyses, having replaced the photoluminescence spectra by photocatalytic activity tests (2). The green background of the diagrams (2) highlights the improvement of NP properties by silica-protected calcination.

dispersions (Fig. S2b, case II.†) was connected upstream of the forced microparticle assembly *via* spray-drying. If the negatively charged silica NPs self-assemble around the sinter-labile NP type, the chance of an ideal separation of these NPs from each other within the supraparticle is increased. Furthermore, differences in NP size should no longer induce a segregation of the two NP types within the spray-dried supraparticles. Thus, an efficient separation of the sinter-labile NPs is guaranteed as long as the silica displays the higher particle number and the smaller particle size in order to form the outer layer during the SLSA[33] (which is shown for CaF_2 and two sizes of silica NPs in varying weight ratios in Fig. S4 and S5 in the ESI†). The process flowsheet of the continuous double assembly of Eu^{3+} containing CaF_2 as exemplary sinter-labile NPs with silica NPs is shown in Fig. 2a (and Experimental details can be found in the ESI†). The aqueous silica and CaF_2 sols are pumped into a static mixer in a NP weight ratio of 9 : 1. This results in a dispersion of well-separated silica NPs of around 20 to 30 nm in size and soft-agglomerates of CaF_2 NPs of around 200 nm (Fig. 2b1 and b2). Ultrasound application enables the SLSA of silica NPs around the CaF_2 NPs yielding soft-agglomerates of around 100 nm in size besides well-separated silica NPs due to their number surplus (Fig. 2c1 and c2). Subsequent spray-drying provides nanostructured microparticles consisting of CaF_2 NPs embedded into silica NPs (Fig. 2d). This supraparticle structure enables the calcination without hard-agglomeration to bulk lumps up to at least 800 °C (Fig. S6 in the ESI† in comparison to spray-dried CaF_2 NPs without silica protection).

In order to highlight the benefits of the silica-protected calcination route, the properties of the obtained Eu^{3+} containing CaF_2 NPs after calcination at 600 °C were compared to the as synthesized CaF_2 crystals (Fig. 3a and b). While the rare-earth luminescence is significantly enhanced by the calcination, the crystallite size calculated from X-ray diffraction (XRD), using the Scherrer equation, is only slightly increased from 21 ± 3 nm to 26 ± 1 nm. TEM and DLS measurements also confirm the nanoscale sizes of the single-crystalline particle samples. While the measured NP size on TEM micrographs increases from 28 to 46 nm (Fig. S7 in the ESI†), the agglomerate size around 100 nm obtained from DLS shows the dispersion state of the samples in water and indicates soft-agglomeration of the nanoparticles. This soft-agglomeration also complicates the particle size determination *via* TEM. The increase in size shown by TEM and XRD indicates a slight sintering due to coalescence. However, the nanoscale size and nano-redispersibility of the sample are maintained.

Via transfer of the silica-protected calcination route to anatase NPs (Fig. 3c) by adaptation of the silica NP size and amount, the easy portability of this process to other NP materials could be shown. Similar to the calcined silica-protected CaF_2 NPs, the obtained single-crystalline TiO_2 sample displays nanoparticulate size; the crystallite and TEM size only slightly increase from 6 ± 1 nm to 7 ± 1 nm and from 6 to 10 nm, respectively (Fig. 3d, while calcination without silica protection results in bulk material – Fig. S7 in the ESI†). However, the photocatalytic activity is significantly enhanced by the calcination process.

Conclusions

In summary, a silica-protected calcination route for NPs, which prevents their hard-agglomeration to bulk lumps, using supraparticles as intermediary structures was herein presented. This procedure is straight forward, upscalable and readily transferable to almost any kind of metal oxide NP system yielding a significant improvement of properties while maintaining their nanoscale size.

Conflicts of interest

There are no conflicts to declare.

Acknowledgements

This work was financially supported by BMBF NanoMatFutur grant 03XP0149, which is gratefully acknowledged. We thank Tobias Kraus (INM – Leibniz Institute for New Materials) and Louis Weber (INM) for the acquisition of TEM micrographs.

Notes and references

1 Y. X. Pang and X. Bao, Influence of Temperature, Ripening Time and Calcination on the Morphology and Crystallinity of Hydroxyapatite Nanoparticles, *J. Eur. Ceram. Soc.*, 2003, **23**, 1697–1704, DOI: 10.1016/S0955-2219(02)00413-2.

2 D. Deng and J. Y. Lee, Hollow Core–Shell Mesospheres of Crystalline SnO_2 Nanoparticle Aggregates for High Capacity Li + Ion Storage, *Chem. Mater.*, 2008, **20**, 1841–1846, DOI: 10.1021/cm7030575.

3 A. S. Karakoti, P. Munusamy, K. Hostetler, V. Kodali, S. Kuchibhatla, G. Orr, J. G. Pounds, J. G. Teeguarden, B. D. Thrall and D. R. Baer, Preparation and Characterization Challenges to Understanding Environmental and Biological Impacts of Nanoparticles, *Surf. Interface Anal.*, 2012, **44**, 882–889, DOI: 10.1002/sia.5006.

4 Z. Pei, H. Xu and Y. Zhang, Preparation of Cr_2O_3 Nanoparticles *via* C_2H_5OH Hydrothermal Reduction, *J. Alloys Compd.*, 2009, **468**, L5–L8, DOI: 10.1016/j.jallcom.2007.12.086.

5 M. Hamadanian, A. Reisi-Vanani and A. Majedi, Synthesis, Characterization and Effect of Calcination Temperature on Phase Transformation and Photocatalytic Activity of Cu,S-codoped TiO_2 Nanoparticles, *Appl. Surf. Sci.*, 2010, **256**, 1837–1844, DOI: 10.1016/j.apsusc.2009.10.016.

6 F. Gu, S. F. Wang, M. K. Lü, G. J. Zhou, S. W. Liu, D. Xu and D. R. Yuan, Effect of Dy^{3+} Doping and Calcination on the Luminescence of ZrO_2 Nanoparticles, *Chem. Phys. Lett.*, 2003, **380**, 185–189, DOI: 10.1016/j.cplett.2003.09.011.

7 H. Yang, Y. Hu, X. Zhang and G. Qiu, Mechanochemical Synthesis of Cobalt Oxide Nanoparticles, *Mater. Lett.*, 2004, **58**, 387–389, DOI: 10.1016/S0167-577X(03)00507-X.

8 L. K. H. Pallon, R. T. Olsson, D. Liu, A. M. Pourrahimi, M. S. Hedenqvist, A. T. Hoang, S. Gubanski and U. W. Gedde, Formation and the Structure of Freeze-dried

MgO Nanoparticle Foams and their Electrical Behaviour in Polyethylene, *J. Mater. Chem. A*, 2015, **3**, 7523–7534, DOI: 10.1039/C4TA06362G.

9 H. Huang, G. Q. Xu, W. S. Chin, L. M. Gan and C. H. Chew, Synthesis and Characterization of Eu:Y_2O_3 Nanoparticles, *Nanotechnology*, 2002, **13**, 318–323, DOI: 10.1088/0957-4484/13/3/316.

10 D.-W. Kim, D.-S. Kim, Y.-G. Kim, Y.-C. Kim and S.-G. Oh, Preparation of Hard Agglomerates Free and Weakly Agglomerated Antimony Doped Tin Oxide (ATO) Nanoparticles by Coprecipitation Reaction in Methanol Reaction Medium, *Mater. Chem. Phys.*, 2006, **97**, 452–457, DOI: 10.1016/j.matchemphys.2005.08.046.

11 J.-N. Park, A. J. Forman, W. Tang, J. Cheng, Y.-S. Hu, H. Lin and E. W. McFarland, Highly Active and Sinter-resistant Pd-nanoparticle Catalysts Encapsulated in Silica, *Small*, 2008, **4**, 1694–1697, DOI: 10.1002/smll.200800895.

12 J.-N. Park, P. Zhang, Y.-S. Hu and E. W. McFarland, Synthesis and Characterization of Sintering-resistant Silica-encapsulated Fe_3O_4 Magnetic Nanoparticles Active for Oxidation and Chemical Looping Combustion, *Nanotechnology*, 2010, **21**, 225708, DOI: 10.1088/0957-4484/21/22/225708.

13 L. Shang, T. Bian, B. Zhang, D. Zhang, L.-Z. Wu, C.-H. Tung, Y. Yin and T. Zhang, Graphene-Supported Ultrafine Metal Nanoparticles Encapsulated by Mesoporous Silica: Robust Catalysts for Oxidation and Reduction Reactions, *Angew. Chem.*, 2014, **126**, 254–258, DOI: 10.1002/ange.201306863.

14 Y. Dai, B. Lim, Y. Yang, C. M. Cobley, W. Li, E. C. Cho, B. Grayson, P. T. Fanson, C. T. Campbell, Y. Sun and Y. Xia, A Sinter-Resistant Catalytic System Based on Platinum Nanoparticles Supported on TiO_2 Nanofibers and Covered by Porous Silica, *Angew. Chem.*, 2010, **49**, 8165–8168, DOI: 10.1002/anie.201001839.

15 I. Lee, Q. Zhang, J. Ge, Y. Yin and F. Zaera, Encapsulation of Supported Pt Nanoparticles with Mesoporous Silica for Increased Catalyst Stability, *Nano Res.*, 2011, **4**, 115–123, DOI: 10.1007/s12274-010-0059-8.

16 V. Sudheeshkumar, A. Shivhare and R. W. J. Scott, Synthesis of Sinter-resistant Au@silica Catalysts Derived from Au 25 Clusters, *Catal. Sci. Technol.*, 2017, **7**, 272–280, DOI: 10.1039/C6CY01822J.

17 K.-T. Li, M.-H. Hsu and I. Wang, Palladium Core–Porous Silica Shell-Nanoparticles for Catalyzing the Hydrogenation of 4-Carboxybenzaldehyde, *Catal. Commun.*, 2008, **9**, 2257–2260, DOI: 10.1016/j.catcom.2008.05.012.

18 N. M. Wichner, J. Beckers, G. Rothenberg and H. Koller, Preventing Sintering of Au and Ag Nanoparticles in Silica-based Hybrid Gels Using Phenyl Spacer Groups, *J. Mater. Chem.*, 2010, **20**, 3840, DOI: 10.1039/c000105h.

19 S. H. Joo, J. Y. Park, C.-K. Tsung, Y. Yamada, P. Yang and G. A. Somorjai, Thermally Stable Pt/Mesoporous Silica Core–Shell Nanocatalysts for High-temperature Reactions, *Nat. Mater.*, 2009, **8**, 126–131, DOI: 10.1038/nmat2329.

20 L. Shang, H. Yu, X. Huang, T. Bian, R. Shi, Y. Zhao, G. I. N. Waterhouse, L.-Z. Wu, C.-H. Tung and T. Zhang, Well-Dispersed ZIF-Derived Co,N-Co-doped Carbon Nanoframes through Mesoporous-Silica-Protected Calcination as Efficient Oxygen Reduction Electrocatalysts, *Adv. Mater.*, 2016, **28**, 1668–1674, DOI: 10.1002/adma.201505045.

21 D. Sarkar, D. Sen, B. K. Nayak, S. Mazumder and A. Ghosh, Spray-Dried Encapsulated Starch and Subsequent Synthesis of Carbon-Silica Core–Shell Micro-Granules, *Colloids Surf., A*, 2017, **529**, 696–704, DOI: 10.1016/j.colsurfa.2017.06.054.

22 D. Li, N. Poudyal, V. Nandwana, Z. Jin, K. Elkins and J. P. Liu, Hard Magnetic FePt Nanoparticles by Salt-matrix Annealing, *J. Appl. Phys.*, 2006, **99**, 08E911, DOI: 10.1063/1.2166597.

23 S. Wintzheimer, T. Granath, M. Oppmann, T. Kister, T. Thai, T. Kraus, N. Vogel and K. Mandel, Supraparticles: Functionality from Uniform Structural Motifs, *ACS Nano*, 2018, **12**, 5093–5120, DOI: 10.1021/acsnano.8b00873.

24 E. Piccinini, D. Pallarola, F. Battaglini and O. Azzaroni, Self-limited Self-assembly of Nanoparticles into Supraparticles: Towards Supramolecular Colloidal Materials by Design, *Mol. Syst. Des. Eng.*, 2016, **1**, 155–162, DOI: 10.1039/C6ME00016A.

25 Y. Xia, T. D. Nguyen, M. Yang, B. Lee, A. Santos, P. Podsiadlo, Z. Tang, S. C. Glotzer and N. A. Kotov, Self-Assembly of Self-Limiting Monodisperse Supraparticles from Polydisperse Nanoparticles, *Nat. Nanotechnol.*, 2011, **6**, 580–587, DOI: 10.1038/nnano.2011.121.

26 A. B. D. Nandiyanto and K. Okuyama, Progress in Developing Spray-Drying Methods for the Production of Controlled Morphology Particles: From the Nanometer to Submicrometer Size Ranges, *Adv. Powder Technol.*, 2011, **22**, 1–19, DOI: 10.1016/j.apt.2010.09.011.

27 A. Flegler, S. Koch, M. Schneider, C. Gellermann and K. Mandel, in *Handbook of nanomaterials for industrial applications*, Elsevier, Amsterdam, Netherlands, 2018.

28 M. Oppmann, M. Wozar, J. Reichstein and K. Mandel, Reusable Superparamagnetic Raspberry-Like Supraparticle Adsorbers as Instant Cleaning Agents for Ultrafast Dye Removal from Water, *ChemNanoMat*, 2018, **6**, 141, DOI: 10.1002/cnma.201800490.

29 S. Zellmer, G. Garnweitner, T. Breinlinger, T. Kraft and C. Schilde, Hierarchical Structure Formation of Nanoparticulate Spray-Dried Composite Aggregates, *ACS Nano*, 2015, **9**, 10749–10757, DOI: 10.1021/acsnano.5b05220.

30 R. Balgis, L. Ernawati, T. Ogi, K. Okuyama and L. Gradon, Controlled Surface Topography of Nanostructured Particles Prepared by Spray-Drying Process, *AIChE J.*, 2017, **63**, 1503–1511, DOI: 10.1002/aic.15682.

31 F. Iskandar, H. Chang and K. Okuyama, Preparation of Microencapsulated Powders by an Aerosol Spray Method and their Optical Properties, *Adv. Powder Technol.*, 2003, **14**, 349–367, DOI: 10.1163/15685520360685983.

32 J. P. Brunelle, Preparation of Catalysts by Metallic Complex Adsorption on Mineral Oxides, *Pure Appl. Chem.*, 1978, **50**, 1211–1229.

33 M. Maas, C. C. Silvério, J. Laube and K. Rezwan, Electrostatic Assembly of Zwitterionic and Amphiphilic Supraparticles, *J. Colloid Interface Sci.*, 2017, **501**, 256–266, DOI: 10.1016/j.jcis.2017.04.076.